Slip at High Shear Rates

Ashlie Martini,[1] Hua-Yi Hsu,[2] Neelesh A. Patankar,[2] and Seth Lichter[2,*]

[1]*School of Mechanical Engineering, Purdue University, West Lafayette, Indiana 47907, USA*
[2]*Department of Mechanical Engineering, Northwestern University, Evanston, Illinois 60208, USA*

(Received 18 February 2008; published 21 May 2008)

There are contradictory published data on the behavior of fluid slip at high shear rates. Using three methodologies (molecular dynamics simulations, an analytical theory of slip, and a Navier-Stokes-based calculation) covering a range of fluids (bead-spring liquids, polymer solutions, and ideal gas flows) we show that as shear rate increases, the amount of slip, as measured by the slip length, asymptotes to a constant value. The results clarify the molecular mechanics of how slip occurs. Furthermore, they indicate that in this limit, molecular dynamics simulations must accurately account for heat transfer to the solid.

DOI: 10.1103/PhysRevLett.100.206001 PACS numbers: 83.50.Rp, 47.61.−k, 83.10.Rs

Recent experimental, numerical and analytical results show that the fluid adjacent to a solid will have a nonzero net speed relative to the solid [1,2]. Although this slip was speculated from the earliest days of fluid mechanics, its small magnitude made it difficult to substantiate (see the references in [3]). Over the past decade, slip has been amply demonstrated as computational and experimental techniques have improved [4,5]. For nanoscale flows, slip is potentially of technological utility. Small size leads to large flow resistance and hence large energy costs for pumping liquids through nanochannels in processes such as desalination and other chemical purification techniques. However, if the liquid can be made to slip, then the resistance and the energy requirements can be reduced, with the promise that these techniques may be economically viable [6–10]. In another arena, any machine with rotating shafts, bearings, or sliders will have to contend with flow in the small lubricated gaps between two parts in relative motion. As speeds increase and tolerances are reduced, the shear in these gaps increases, and the potential benefits of slip for inculcating better lubrication and reduced wear becomes significant [11,12].

There is no consensus on the high-shear rate behavior of slip. Molecular dynamics (MD) simulation studies can be divided broadly into two categories: those that predict unbounded slip length at high shear rates [11,13–15] and those that do not [16–20]. (For some of these citations, slip length was not reported but was calculable from another reported measure of slip magnitude.) Although all of these studies used nonequilibrium MD simulations in a planar Couette geometry, there is one significant simulation parameter that differentiates the two groups: the wall model. In the simulations that predict unbounded slip length, the walls are rigid: the wall atoms are fixed, and therefore do not have thermal motion. Simulations that predict bounded slip length at high shear rate employ a different wall model in which the wall atoms can oscillate about their equilibrium position in response to collisions with the fluid molecules. We call these flexible walls. A common approach to implement flexible walls is to tether the wall atoms to lattice sites via a linear spring model, thus allowing them to move and interact while maintaining sufficient rigidity to contain the fluid molecules.

The primary goal of this Letter is to provide insight into the underlying atomic-scale physics that leads to slip in the high-shear rate limit. We report on the high-shear rate slip as predicted by three methodologies: MD simulation, dynamical modeling, and continuum fluid dynamics. The techniques cover a range of conditions: a polymer solution, a linear approximation to a simple Lennard-Jones liquid, and an ideal gas. Yet, the three techniques predict the same slip behavior in the high-shear limit: an approach to a constant slip length. We show that previous reports of unbounded slip arise from neglecting momentum transfer between the fluid and the solid. We finally show that controlling the temperature in MD simulations by applying a numerical thermostat to the fluid will yield the incorrect slip in the high-shear rate limit.

We start our investigation of high-shear slip behavior using MD simulation. Our simulations consisted of *n*-decane molecules sheared in a Couette flow in which the upper and lower walls were moved at equal and opposite speeds $\pm U$ between 3.2 and 1000 m/s. The walls consisted of atoms forming four planes of a face-centered-cubic lattice. The channel height h, defined as the distance between the mean center of mass of the innermost wall atoms, was 3 nm. Periodic boundary conditions were applied in the flow direction and transverse to the wall-normal direction. The *n*-decane molecules were simulated using a united atom model (i.e. each molecule is composed of ten monomers connected by rigid bonds) and allowing for both bond bending and torsion. The liquid density (96 *n*-decane molecules) was determined using a grand canonical (i.e., constant temperature, volume, chemical potential) Monte Carlo simulation where the liquid is allowed to reach equilibrium in a way that models the density which would be present if the channel were filled from a constant temperature reservoir. Following equilibration, simulations were run with a time step of 10^{-6} ns to a minimum duration of 1 ns.

 © 2008 The American Physical Society

All nonbonded interactions were modeled using Lennard-Jones potentials parametrized by energy ϵ and length σ. For interactions between two atoms of the same type, the length parameters were $\sigma_{CH_3} = 0.377$ nm, $\sigma_{CH_2} = 0.393$ nm, and $\sigma_{wall} = 0.266$ nm, and the energy parameters were $\epsilon_{CH_3}/k_b = 98.1$ K, $\epsilon_{CH_2}/k_b = 47.0$ K, and $\epsilon_{wall}/k_b = 529.3$ K. Parameters for interactions between different atom types were calculated using the Lorentz-Berthelot mixing rules.

Two sets of simulations were run using the above parameters: rigid walls with a thermostat applied to the liquid atoms, and flexible walls with only the wall atoms subject to the thermostat. In the rigid wall case, the wall atoms were held at their lattice site locations. The fixed wall atoms did not vibrate, could not conduct heat, and therefore the simulation temperature was controlled by thermostatting the liquid atoms. For the second set of simulations, each wall atom was tethered to its lattice site by a linear spring. For this flexible wall, heat generated within the liquid was conducted to the walls through atom-atom interactions and then removed via a thermostat applied to the wall atoms [21]. Efficient and stable heat conduction was optimized in our simulations by a spring constant of $3.19\,\sigma^2_{wall}/\epsilon_{wall}$. In all cases, the temperature of the thermostatted atoms was maintained at 300 K using a Nosé-Hoover thermostat. Additional simulation detail is in [22].

The mean shear rate $\dot{\gamma}$ was determined by fitting a straight line to the average velocity profile in the central part of the channel. One measure of slip is the slip speed v_s defined as the difference between the wall speed and $\dot{\gamma}$ extrapolated to the wall. It is more usual to report the extent of slip by using the slip length $L_s \equiv v_s/\dot{\gamma}$.

The slip length determined from our MD simulations is shown in Fig. 1. For the case of a rigid wall, slip length becomes unbounded as wall speed is increased. For a flexible wall, the slip length approaches a constant value at high shear rates.

The slip behavior is now evaluated using an approximate solution to a dynamical model which we previously introduced [20,23]. The model is a simple force balance tangent to the wall,

$$m\ddot{x}_i = -\frac{2\pi g}{\lambda}\sin\left(\frac{2\pi x_i}{\lambda}\right) + k(x_{i+1} - 2x_i + x_{i-1}) + \eta_{LL}(V - \dot{x}_i) - \eta_{LS}\dot{x}_i, \quad (1)$$

in which the acceleration $\ddot{x}_i$ of the ith atom of mass m along the shear direction is due to (i) the force of magnitude g arising from the linear array of solid atoms with spacing λ, (ii) the interactions of strength k from the nearest-neighbor liquid atoms at $i + 1$ and $i - 1$, (iii) the force due to shear from the liquid layer above which is moving at speed $V = \dot{\gamma}(h/2 - 2d)$ where d is the liquid-liquid spacing normal to the surface, and finally, (iv) the frictional force, with coefficient η_{LS}, due to slip along the wall. The coefficient $\eta_{LL} \equiv \eta(\mathcal{A}/d)/N$ is the bulk viscosity η times a coefficient to apportion the continuum viscosity coefficient to the discrete liquid atoms, where $\mathcal{A}/N$ is the area per liquid atom adjacent to the wall. Equation (1) is augmented by probabilistic equations normal to the wall, which can remove any atom i or insert atoms in accord with diffusion to and from the bulk [23]. The complete set of equations is called the variable-density Frenkel-Kontorova (VDFK) model. The VDFK model can be solved numerically or approximated analytically [24,25].

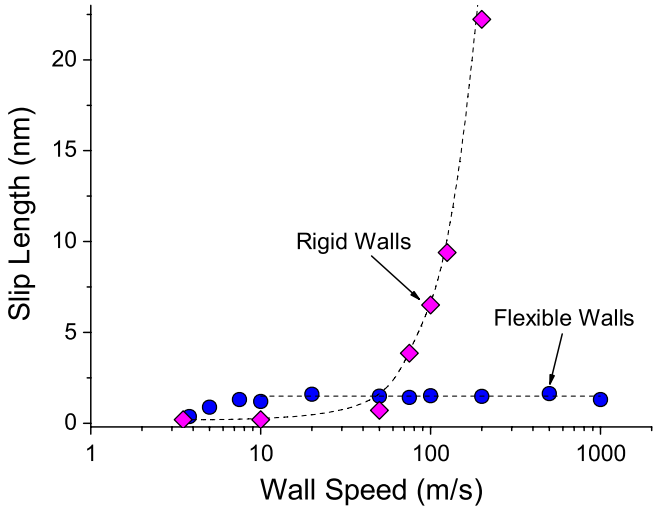

FIG. 1 (color online). Slip length as a function of wall speed. Data points are shown as diamonds for the rigid walls in which the liquid was thermostated; circles are for the case of flexible walls in which the solid was thermostated. The dashed lines are an aid to the eye, in particular, a line of zero slope is fit to the flexible-wall data for $U > 20$ m/s.

At large values of the forcing parameter V, Eq. (1) is dominated by the force due to shear $\eta_{LL}(V - \dot{x}_i)$ and the friction force due to slip along the wall $\eta_{LS}\dot{x}_i$. The dominant balance of these two terms leads to the result, $v_s = \eta_{LL}V/(\eta_{LL} + \eta_{LS})$ where, since all atoms have the same velocity, the individual atomic velocities $\dot{x}_i$ have been replaced by v_s. After using the definition of the slip length, and approximating the shear rate by $\dot{\gamma} = (V - v_s)/d$, we find

$$L_s = \frac{\eta_{LL}}{\eta_{LS}}d. \quad (2)$$

This result corroborates the MD simulation finding shown in Fig. 1 that in the limit of high forcing the slip length asymptotes to a constant value. Furthermore, Eq. (2) predicts that the slip length is inversely proportional to the friction coefficient η_{LS}. Notably, as friction goes to zero, the slip length becomes unbounded. In a MD simulation, the case $\eta_{LS} = 0$ is modeled by curtailing momentum transfer from the fluid to the solid, that is, by enforcing a rigid wall. Hence, in a simulation with rigid walls, Eq. (2) predicts that the slip length will become unbounded as the forcing increases, as seen in Fig. 1.

To describe molecular-scale slip behavior by using continuum equations [26], we note that (i) near the wall, the fluid experiences a potential from the wall molecules, and (ii) the fluid density responds to the wall potential; hence, fluid compressibility is relevant. To incorporate these features, we simulated shear flow of a compressible fluid between two walls in the presence of a wall potential. For low Reynolds numbers, the steady-state form of the conservation of momentum equation for a compressible fluid is

$$-\nabla p + \eta\nabla^2\mathbf{u} + \frac{\eta}{3}\nabla(\nabla\cdot\mathbf{u}) - \rho\nabla\phi = \mathbf{0}, \qquad (3)$$

where $\mathbf{u} = (u, v)$ is the fluid velocity, p is pressure, and ρ is density. Mass conservation is expressed by $\nabla\cdot(\rho\mathbf{u}) = 0$. The ideal gas equation of state, $p = \rho RT$, is used, where R is the gas constant and the temperature T is assumed constant. Shear flow was imposed by applying a given velocity U_t to the top boundary at which the no-slip condition was maintained. Near the bottom boundary, the fluid was subjected to the potential field $\phi = \phi_a e^{-ky}\cos(my)[1.1 + b\sin(mx)]$, where ϕ_a, k, m, and b are parameters [27], and (x, y) are directed tangent and normal to the wall, respectively. The gradient of this potential gives rise to the body force term in Eq. (3). At the bottom wall the Navier boundary condition $\mu\partial u/\partial y = \eta_w u$ was used in the flow direction, where η_w is the friction factor at the wall, and $v = 0$ normal to the wall. This set of equations and boundary conditions was solved numerically for different values of the imposed velocity U_t, and the slip length on the lower wall was obtained as discussed earlier. Figure 2 shows a plot of slip length versus shear rate for different values of the wall friction η_w. The continuum equations capture the form of the slip length behavior as seen in the MD simulations and the VDFK equations, corroborating that the slip length is nearly constant (here nearly zero) at low shear rates and subsequently increasing sharply as shear rate increases. Figure 2 further indicates that the transition from low to high-shear slip behavior occurs at $\dot\gamma \sim \rho\phi_a/\eta$. The physical mechanism of this transition is discussed in the next paragraph. Of relevance here is that at high shear rates, the slip length approaches a constant which is dependent on the value of η_w. After the change of variable $\eta_w = \eta_{LS}(N/\mathcal{A})$, the inset to Fig. 2 shows that the continuum analysis also finds that slip length is inversely proportional to the friction factor, in agreement with Eq. (2). Finally, Fig. 2 shows that if there is no wall friction, the slip length becomes unbounded at high shear rates.

In this Letter, we have analyzed the high-shear rate limit of slip. In the small-shear rate limit $\dot\gamma \to 0$, Green-Kubo analysis [28] provides a means to analyze slip where momentum transfer to the wall is absent and slip is dominated by the amplitude of the potential-energy corrugations due to the lattice of discrete solid atoms. Fluid atoms must overcome the Peierls-Nabarro (PN) barrier due to the

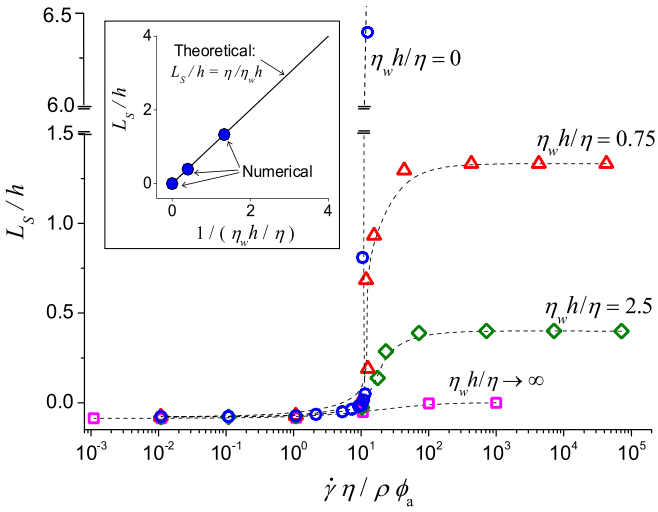

FIG. 2 (color online). The slip length as a function of normalized shear rate predicted from the continuum equations. Data points for different values of the nondimensional friction factor $\eta_w h/\eta$ (□ ∞; ◇ 2.5; △ 0.75; ○ 0) are connected by dashed lines as an aid to the eye. For finite values of the friction between the fluid and the wall, the slip length approaches a constant value in the high-shear limit. This constant value depends inversely on the friction factor as predicted by the VDFK model, Eq. (2), as shown in the inset.

difference between stable and unstable equilibrium-state energies [20,23,29]. As shear rate increases, and the speed of the slipping atoms increases, fluid atoms do not invaginate themselves into the lower levels of the solid potential, but rather skim over the substrate. Hence, the effective roughness decreases and the resistance to slip also vanishes [13,30]. Realistically, though, collisions of fluid atoms with the wall atoms transfer momentum to the walls. For a collision between a fluid and a solid atom of mass ratio M, the exit speed $\mathcal{V}_e$ of the fluid atom after the collision will be some fraction $\Omega(M, \alpha)$ of the incident speed $\mathcal{V}$, $\mathcal{V}_e = \Omega(M, \alpha)\mathcal{V}$, where α is the impact angle. Consequently, the momentum lost by the fluid atom, which is also proportional to its speed, is transferred to the solid atom. Unlike the PN-dominated slip at low shear described by the Green-Kubo analysis, we have shown that this momentum transfer dominates the high-shear rate dynamics of slip. Momentum transfer is incorporated into an MD simulation by using a flexible wall, into the VDFK model through the term $\eta_{LS}\dot{x}$, and into the continuum equations through the wall friction parameter $\eta_w u$. This term in the VDFK and continuum equations is purely frictional; i.e., it does not model other roles that a flexible wall may play in an MD simulation, for example, that the oscillatory motion of the solid atoms may transfer energy back into the fluid and affect its dynamics. The concurrence of the three techniques in predicting an asymptotic approach to a constant slip length indicates that momentum transfer resulting in frictional dissipation is of primary importance.

The value of investigating a limiting behavior is that a single mechanism dominates all others: differences in the predictions from alternative possible mechanisms are accentuated which helps identify which is correct. Unlike in the low-shear limit, we find that, whether for a polymer melt or an ideal gas, friction is the dominant force as shear rate becomes large. Accounting for this force yields the result that the high-shear rate slip length does not become unbounded, as previously thought, but rather approaches a constant value. Finally, we show that momentum transfer to the solid needs to be part of an MD simulation of slip at high shear rates.

Momentum transfer at the wall can be expected to be more complex than that expressed by the constant friction coefficient used in the VDFK and continuum models. Yet, even with this simplification, these models agree with the MD simulation findings presented above. At shear rates even higher than those presented here, above the sound speed of the solid, our models may need to be amended. These possible complications may be viewed with some optimism. Unlike the no-slip boundary condition which is material independent, the dependence of slip on the material properties of the solid may point to new ways to control fluids, which are not available for flows which adhere to the no-slip condition.

This work was partially supported by the National Center for Supercomputing Applications under No. TG-MSS070031N and utilized the NCSA Xeon Linux Supercluster. N. A. P. and H. Y. H. were partially funded by National Science Foundation through the CAREER Grant No. CTS-0134546.

*Corresponding author.
s-lichter@northwestern.edu

[1] L. Bocquet and J.-L. Barrat, Soft Matter **3**, 658 (2007).
[2] Y. Zhu and S. Granick, Phys. Rev. Lett. **87**, 096105 (2001).
[3] E. Lauga, M. P. Brenner, and H. A. Stone, in *Handbook of Experimental Fluid Dynamics*, edited by J. Foss, C. Tropea, and A. Yarin (Springer, New York, 2005), Chap. 15.
[4] J. Koplik, J. R. Banavar, and J. F. Willemsen, Phys. Fluids A **1**, 781 (1989).
[5] C. Neto, D. R. Evans, E. Bonaccurso, H.-J. Butt, and V. S. J. Craig, Rep. Prog. Phys. **68**, 2859 (2005).
[6] J. K. Holt, H. G. Park, Y. Wang, M. Stadermann, A. B. Artyukhin, C. P. Grigoropoulos, A. Noy, and O. Bakajin, Science **312**, 1034 (2006).
[7] M. Majumder, N. Chopra, R. Andrews, and B. J. Hinds, Nature (London) **438**, 44 (2005).
[8] M. Urbakh, J. Klafter, D. Gourdon, and J. Israelachvili, Nature (London) **430**, 525 (2004).
[9] D. S. Sholl and J. K. Johnson, Science **312**, 1003 (2006).
[10] J. C. T. Eijkel and A. van den Berg, Microfluid. Nanofluid. **1**, 249 (2005).
[11] Y. Chen, D. Li, K. Jiang, J. Yang, X. Wang, and Y. Wang, J. Chem. Phys. **125**, 084702 (2006).
[12] J. Gao, W. D. Luedtke, and U. Landman, Tribol. Lett. **9**, 3 (2000).
[13] P. A. Thompson and S. M. Troian, Nature (London) **389**, 360 (1997).
[14] N. V. Priezjev and S. M. Troian, Phys. Rev. Lett. **92**, 018302 (2004).
[15] R. S. Voronov, D. V. Papavassiliou, and L. L. Lee, J. Chem. Phys. **124**, 204701 (2006).
[16] A. Jabbarzadeh, J. D. Atkinson, and R. I. Tanner, J. Non-Newtonian Fluid Mech. **77**, 2612 (1998).
[17] R. Khare, J. J. de Pablo, and A. Yethiraj, Macromolecules **29**, 7910 (1996).
[18] S. A. Gupta, H. D. Cochran, and P. T. Cummings, J. Chem. Phys. **107**, 10 316 (1997).
[19] N. V. Priezjev, J. Chem. Phys. **127**, 144708 (2007).
[20] A. Martini, A. Roxin, R. Q. Snurr, Q. Wang, and S. Lichter, J. Fluid Mech. **600**, 257 (2008).
[21] U. Heinbuch and J. Fischer, Phys. Rev. A **40**, 1144 (1989).
[22] A. Martini, Y. C. Liu, R. Q. Snurr, and Q. Wang, Tribol. Lett. **21**, 217 (2006).
[23] S. Lichter, A. Roxin, and S. Mandre, Phys. Rev. Lett. **93**, 086001 (2004).
[24] O. M. Braun and Y. S. Kivshar, Phys. Rep. **306**, 1 (1998).
[25] A. Roxin, Ph.D. thesis, Northwestern University, 2004.
[26] N. A. Patankar and H.-Y. Hsu, in Proceedings of the 60th Annual Meeting of the Division of Fluid Dynamics of the American Physical Society, Salt Lake City, Utah, 2007 (unpublished).
[27] W. A. Steele, Surf. Sci. **36**, 317 (1973).
[28] J.-L. Barrat and L. Bocquet, Faraday Discuss. **112**, 119 (1999).
[29] S. Lichter, A. Martini, R. Q. Snurr, and Q. Wang, Phys. Rev. Lett. **98**, 226001 (2007).
[30] N. V. Priezjev and S. M. Troian, J. Fluid Mech. **554**, 25 (2006).